Chemical Science

ROYAL SOCIETY OF CHEMISTRY

EDGE ARTICLE

View Article Online
View Journal | View Issue

Cite this: *Chem. Sci.*, 2023, **14**, 9892

All publication charges for this article have been paid for by the Royal Society of Chemistry

Received 25th April 2023
Accepted 24th August 2023

DOI: 10.1039/d3sc02117c

rsc.li/chemical-science

A high-field cellular DNP-supported solid-state NMR approach to study proteins with sub-cellular specificity†

David Beriashvili, [a] Ru Yao, [b] Francesca D'Amico, [c] Michaela Krafčíková, [a] Andrei Gurinov, [a] Adil Safeer,[a] Xinyi Cai,[b] Monique P. C. Mulder, [c] Yangping Liu, [b] Gert E. Folkers[a] and Marc Baldus *[a]

Studying the structural aspects of proteins within sub-cellular compartments is of growing interest. Dynamic nuclear polarization supported solid-state NMR (DNP-ssNMR) is uniquely suited to provide such information, but critically lacks the desired sensitivity and resolution. Here we utilize SNAPol-1, a novel biradical, to conduct DNP-ssNMR at high-magnetic fields (800 MHz/527 GHz) inside HeLa cells and isolated cell nuclei electroporated with [^{13}C,^{15}N] labeled ubiquitin. We report that SNAPol-1 passively diffuses and homogenously distributes within whole cells and cell nuclei providing ubiquitin spectra of high sensitivity and remarkably improved spectral resolution. For cell nuclei, physical enrichment facilitates a further 4-fold decrease in measurement time and provides an exclusive structural view of the nuclear ubiquitin pool. Taken together, these advancements enable atomic interrogation of protein conformational plasticity at atomic resolution and with sub-cellular specificity.

Introduction

Organelles are physiochemically distinct microenvironments tuned to efficiently execute biological processes.[1–3] Recent technological advancements have made rapid *in situ* whole-cell and organelle-specific protein interactome mapping with nanometer resolution possible.[4–6] The next step in deepening our knowledge of these processes lies in gathering organelle-specific atomic-level structural data.

Nuclear magnetic resonance (NMR) provides atomic-resolution data and is amenable for application *in situ*. Prominently, solution-state NMR has been used to characterize rapidly tumbling or intrinsically disordered biomolecules within intact eukaryotic cells and isolated mitochondria.[7–12] To overcome tumbling limitations, magic angle spinning (MAS) solid-state NMR (ssNMR), has been applied to probe abundant globular proteins,[13] soluble as well membrane-embedded proteins in bacteria,[14,15] and protein-enriched eukaryotic membrane vesicles.[16]

Overcoming sensitivity limitations in ssNMR is increasingly possible by application of dynamic nuclear polarization (DNP) based-ssNMR (DNP-ssNMR),[17] which greatly increases sensitivity by transferring electron polarization from carefully chosen biradical polarization agents (PAs) to NMR active nuclei. It has already allowed to determine the supramolecular structure of native diatom biosilica as well as to visualize structural elements of and binding events to supra-protein complexes embedded in native-membranes derived from both bacteria and human cells.[16,18,19] Moreover, DNP-ssNMR has been applied to cell lysates,[20,21] eukaryotic cells grown as 2D or 3D cultures,[22–24] and to soluble proteins in bacteria[15] and within eukaryotic cells at near endogenous (μM) concentrations.[25] In spite of these advancements, our current knowledge regarding line-broadening effects under low temperature-DNP conditions stems from *in vitro* preparations where inhomogeneous broadening usually dominates and correlates with local protein dynamics,[26–29] resulting in narrow line widths for rigid protein segments and broader distributions for mobile or surface exposed residues.[26,27,30,31]

However, all these applications have been limited to DNP setups operating at comparatively low magnetic field (400 MHz/600 MHz).[20,22,24,25] Extending such experiments to higher magnetic fields has been complicated by a lack of suitable PAs.[22,23] Secondly, obtaining detailed information regarding the penetration and distribution of PAs within whole cells is crucial for correlating in-cell DNP-ssNMR readouts with sub-cellular localization. Lastly, further complications may arise in cells where the surrounding physio–chemical environment varies in

[a]*NMR Spectroscopy, Bijvoet Center for Biomolecular Research, Utrecht University, Padualaan 8, 3584 CH Utrecht, The Netherlands. E-mail: m.baldus@uu.nl*

[b]*Tianjin Key Laboratory on Technologies Enabling Development of Clinical Therapeutics and Diagnostics, School of Pharmacy, Tianjin Medical University, Tianjin 300070, P. R. China*

[c]*Department of Cell and Chemical Biology, Leiden University Medical Center (LUMC), Einthovenweg 20, 2333 ZC, Leiden, The Netherlands*

† Electronic supplementary information (ESI) available. See DOI: https://doi.org/10.1039/d3sc02117c

space and time (see, *e.g.* ref. 32 and 33) leading to additional unfavorable broadening mechanisms that may prohibit a detailed conformational analysis of the protein of interest at low magnetic fields.

Here, we set out to address these issues and to determine whether SNAPol-1, a PA with demonstrated exceptional high-field performance *in vitro*,[34,35] could be efficiently utilized in the context of high-field in cell DNP-ssNMR. Through confocal z-stack microscopy we investigated the distribution of SNAPol-1 in whole cells and cell nuclei. In line with DNP ssNMR data, our findings suggest a homogeneous distribution of PA in both preparations. To confirm confocal data and further probe potential SNAPol-1-related sensitivity and resolution improvements, we conducted high-field (800 MHz) DNP-ssNMR experiments on HeLa cells and isolated nuclei containing [^{13}C,^{15}N] ubiquitin (Ub), a post-translational modifier that regulates a host of cellular functions,[36] delivered by electroporation.[25] Comparison of our high-field in-cell and in nuclei data with in-cell data acquired at 400 MHz and on *in vitro* Ub revealed significant improvement in spectral sensitivity and resolution at 800 MHz DNP conditions thus providing an avenue for broadly studying the conformational landscape of proteins in cells at atomic resolution and with sub-cellular precision.

Results and discussion

It is well established that a PA's DNP performance is highly reliant on it being in close proximity to the molecular species of interest.[24–26,37] To assess SNAPol's suitability for cellular applications we first investigated its ability to passively enter and distribute within mammalian cells. Confocal z-stack microscopy of HeLa cells treated with fluorescein isothiocyanate (FITC) tagged-SNAPol-1 (Fig. S1†) dissolved in "DNP Juice" (6 : 3 : 1 d8 glycerol : D_2O : H_2O) revealed that SNAPol-1 passively entered cells distributing homogenously within the luminal space, similar to PyPOL (Fig. 1A and S2†).[25] Due to its large size (1.6 kDa), we postulate that glycerol-induced membrane-permeability plays a role in facilitating SNAPol-1 entry into cells.[38]

To validate our confocal data, we initially conducted DNP-ssNMR experiments on HeLa cells and later isolated nuclei electroporated with 1.2 mM [^{13}C,^{15}N] Ub. For both type of preparations, we also performed solution-state NMR control experiments (Fig. S3†). These experiments showed signals exclusively for residues in Ub's dynamic C-terminal tail within intact cells in full agreement with published in-cell solution-state NMR data[11,25,39] We also note that these results obtained in at least two different human cell lines are at odds with a recent report from Kadavath *et al.*,[40] possibly due to their use of a non-human cell line. Notably, we did not observe any solution-state NMR correlations for Ub within the intact nuclei (Fig. S3†) in line with a high degree of conjugation of the nuclear Ub pool.[41]

We conducted adiabatic ^{1}H–^{13}C cross polarization (CP) and saturation recovery experiments (Fig. 1B/C) on HeLa cells electroporated with 1.2 mM [^{13}C,^{15}N] Ub, which equates to 40 μM of delivered protein.[25] Doping with 30 mM SNAPol-1 revealed

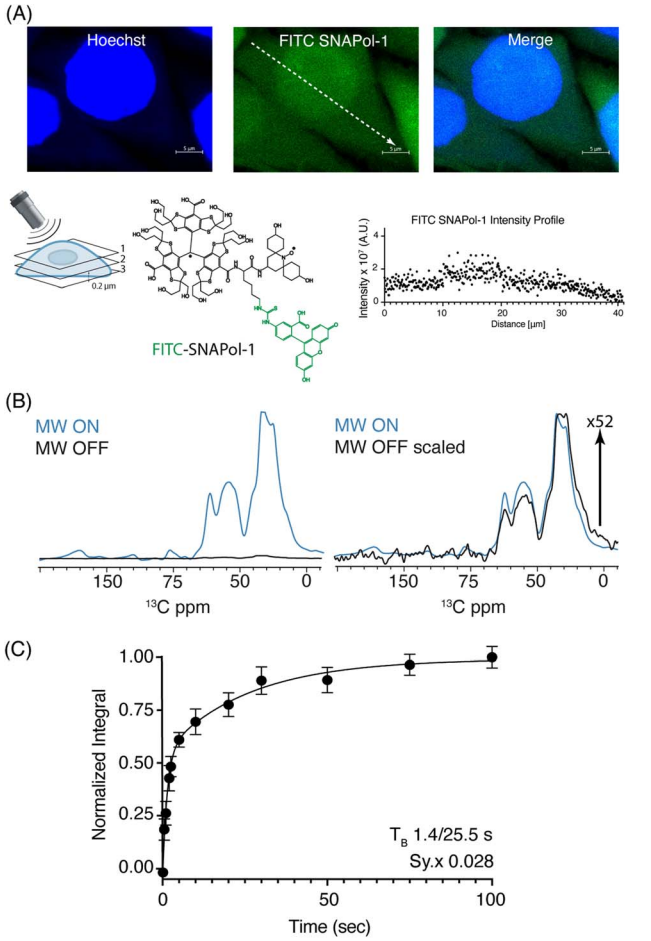

Fig. 1 (A): Confocal z-stack of FITC-SNAPol-1 (green) treated HeLa cells counterstained with Hoechst (blue) along with an illustrative FITC-SNAPol-1 intensity profile taken along the arrow depicted in the green panel. (B/C): SNAPol-1 DNP enhancement on 8 million HeLa cells electroporated with 1.2 mM [^{13}C,^{15}N] Ub treated with 30 mM SNAPol-1 embedded in "DNP Juice" (6 : 4 d8, $^{12}C_3$-enriched glycerol : D_2O with 1 × Hank's buffered salt solution HBSS) as previously described in ref. 25. In (C), polarization buildup (T_B) on the carbonyl signal was best fit by a biexponential with error bars denoting the standard deviation (s.d.) of the signal to noise ratio (S/N) and Sy.x the s.d. residual of the fit. See ESI† for more details on error analysis.

a DNP enhancement of 52 (Table 1), characterized by a biexponential polarization buildup time (T_B) of 1.40/25.5 s with the former accounting for 57% of the buildup.[34] These results are in good agreement with our recent findings for a bioresistant variant (Stapol-1)[35] and suggested the presence of two PA populations. We attribute the fast buildup rate (1.40 s) to lumen-localized SNAPol-1 with the longer (25.5 s) likely arising from SNAPol-1 outside or at the cell's periphery. Comparison of absolute enhancements (Σ) at 800 MHz/527 GHz for proline, revealed that the weighted average Σ for in-cell SNAPol-1 is an order of magnitude greater than reported for AMUPol which was previously used for cellular DNP-ssNMR.[22,24,25] Notably and in line with earlier observations for complex biological systems,[16,22,34] in-cell enhancements decreased compared to *in vitro* SNAPol-1 values recorded on proline.

Table 1 Comparison of absolute enhancements (Σ) obtained at 800 MHz/527 GHz for in-cell SNAPol-1 samples (judged on Ub carbonyl signal – 170 to 185 ppm) *versus in vitro* AMUPol and SNAPol-1 results on 0.25 M proline (6 : 3 : 1 glycerol : D_2O : H_2O). $\varepsilon_{on/off}$, ε_{abs}, and Σ as per convention.[34,43,44] Avg. denotes weighted average Σ (by percent of the fit)

Sample	$\varepsilon_{on/off}$	ε_{abs}	T_B (s)	Σ
SNAPol-1 whole cell (30 mM)	52	45.26	1.4/25.5	340 ± 10/77 ± 7 avg. 229 ± 9
SNAPol-1 nuclei (30 mM)	60	54	1.4	406 ± 19
SNAPol-1 proline (10 mM)[a]	133	116	4.2/3.15	505 ± 7/544 ± 10
AMUPol proline (10 mM)[a]	35	19	5.0	76 ± 8
AMUPol proline (30 mM)[a]	43	23.22	8.2	72 ± 11

[a] Data taken from ref. 34. See ESI for further information.

Next, we investigated improvements in ssNMR resolution at 800 MHz DNP conditions on cells electroporated with 1.2 mM [^{13}C,^{15}N] Ub by recording 3D double-quantum, single-quantum, single-quantum ^{13}C–^{13}C–^{13}C (DQSQSQ)[42] experiments (see ESI for details) using 30 mM SNAPol-1. To examine resolution improvements, we compared these data to Ub in-cell DNP-ssNMR experiments conducted at 400 MHz (30 mM AMUPol, Fig. 2A).

Linewidth analysis of Cα and Cβ correlations corresponding to residues located in various secondary structural elements showed a reduction in linewidth from about 10% (L50) up to 35% for residues such as T7, K33, N60, most likely reflecting different relative contributions of homogeneous and inhomogeneous line broadening.[31,43,45] Cumulatively, the improvement in resolution seen in our 3D data sets enabled the assignments of an additional 16 residues (leading to 41 assigned residues at

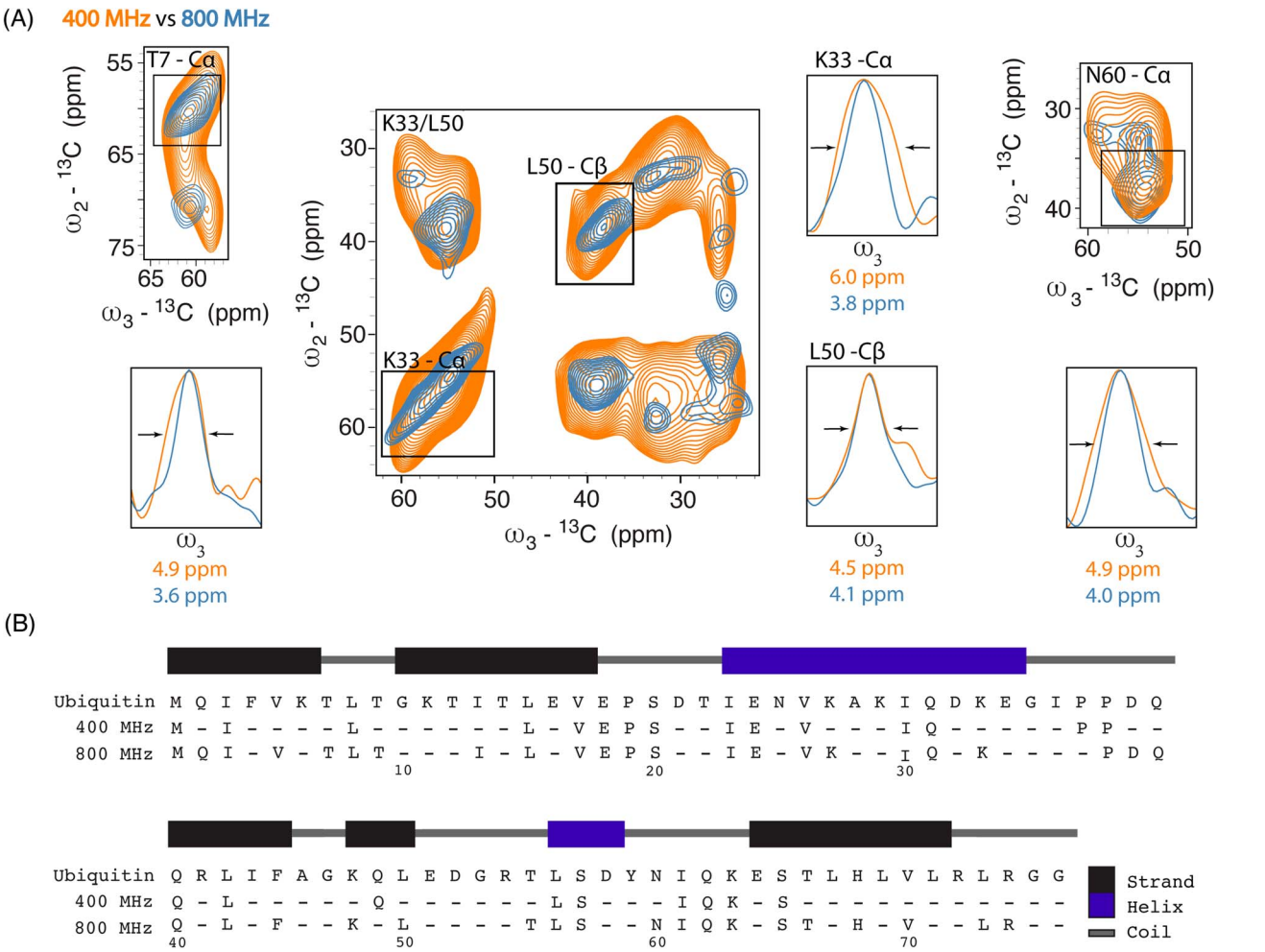

Fig. 2 (A) Overlay of 2D SQSQ planes extracted from ^{13}C–^{13}C–^{13}C DQSQSQ 3D experiments recorded on 8 million HeLa cells electroporated with 1.2 mM [^{13}C,^{15}N] Ub and doped with 30 mM AMUPol, at 400 MHz (orange) and with 30 mM SNAPol-1 at 800 MHz (blue). 1D projections detail linewidth improvement (full width at half maximum (FWHM)). (B) Ubiquitin sequence showing the increase in assignments between Ub in-cell samples measured at 400 (25 residues) and 800 MHz (41 residues) (assignment required 2 or more resolved correlations).

800 MHz) (Fig. 2B) and in a few cases allowed to discern between residues with overlapping chemical shifts (*e.g.*, P37 and P38). Further, comparison of in cell 800 MHz line widths with those obtained on microcrystalline Ub (also recorded at 800 MHz) revealed that while in cell line widths are broader (Fig. S4†), differences varied significantly between residues (36% for T7 and 60% in the case of K33) in line with the dynamic nature of Ub previously found *in vitro* (see, *e.g.*, ref. 46–49). It is important to highlight that variation in line widths could arise from differences in measurement temperatures, chemical exchange (100 K whole cells *vs.* 278 K microcrystals), and that the microcrystals are solely reflective of Ub's free monomeric state. Correspondingly, this comparison serves as a qualitative measure.

Considering the respectable performance of SNAPol-1 at 800 MHz, we proceeded to investigate whether conducting organelle specific DNP-ssNMR was technically feasible. We settled on investigating cell nuclei, isolated *via* a near quantitative detergent nucleus enrichment protocol known to retain transcriptional activity.[50] The rapid nature of isolation afforded by this method would also minimize stress-induced ubiquitinome alterations.[51] Similar to whole cells, confocal z-stack microscopy of FITC-SNAPol-1 treated isolated cell nuclei showed SNAPol-1 entry and homogenous distribution (Fig. 3A and S5†). In addition, we examined whether Ub electroporated into whole cells would be retained upon nuclei isolation. Therefore, we conducted an analogous confocal z-stack microscopy experiment with N-terminal 5-carboxytetramethylrhodamine-tagged Ub (TAMRA-UB), which showed that cell nuclei isolated from whole-cells, electroporated with TAMRA-Ub (Fig. S6†), retained morphology and Ub upon fractionation (Fig. 3B). The lack of TAMRA-Ub in certain locations of the cell nuclei mirrored previously reported results further purporting that the isolation procedure was minimally invasive and retained sub-cellular morphology.[25,52,53] In addition, we tested the suitability of isolated nuclei for DNP ssNMR (*i.e.*, MAS (8 kHz), 60% glycerol, and cryogenic temperature, Fig. S7†) by brightfield microscopy. No adverse effects on morphology were observed in line with earlier studies[54,55] suggesting that transcriptional activity and morphology of isolated nuclei are maintained if stored in high glycerol concentrations (>60%) and at cryogenic temperatures.

DNP-ssNMR adiabatic ^{1}H–^{13}C cross polarization (CP) and saturation recovery experiments conducted on nuclei isolated from HeLa cells electroporated with 1.2 mM [^{13}C,^{15}N] Ub (Fig. 3C/D) and then doped with 30 mM SNAPol-1, exhibited a DNP enhancement of 60, characterized by a short mono-exponential polarization buildup time (T_B) of 1.40 s, confirming that SNAPol-1 was in the vicinity of Ub. In line with this notion, we observed an in-nuclei DNP enhancement Σ (Table 1) of 406 compared to 229 in whole cells, approaching values obtained with SNAPol-1 in proline.

Next, we performed 3D DQSQSQ ^{13}C–^{13}C–^{13}C experiments to visualize Ub's nuclear pool at atomic resolution. A cumulative 1D projection, derived from the SQSQ dimension, showed a 2 fold increase in S/N for both carbonyl and aliphatic signals in-nuclei (Fig. S8†) which we attribute to physical sample enrichment (allowing for increased nuclei packing) and more efficient

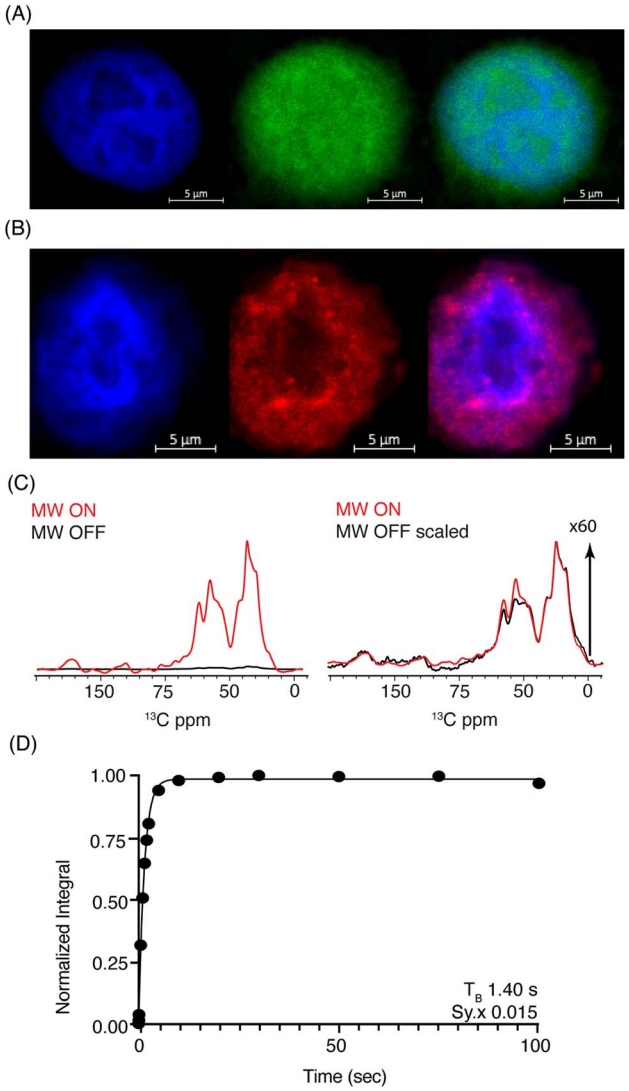

Fig. 3 (A) Confocal z-stack of cell nuclei stained with Hoechst (blue) treated FITC-SNAPol-1 (green). (B) Confocal z-stack of cell nuclei isolated from HeLa cells electroporated with 1.2 mM of TAMRA-Ub (red) stained with Hoechst (blue). Panel (C/D) SNAPol-1 DNP enhancement (judged on Ub carbonyl signal 170 to 185 ppm) on cell nuclei isolated from 16 million HeLa cells electroporated with 1.2 mM [^{13}C,^{15}N] Ub and treated with 30 mM SNAPol-1 dissolved in "DNP Juice" (6 : 4 d8, $^{12}C_3$-enriched glycerol : D_2O with 1 × HBSS) as previously described in ref. 25. Polarization buildup (T_B) on the carbonyl signal was best fit by a mono-exponential with Sy.x denoting the residual s.d. of the fit. Error bars are not visible due to high S/N ratio. See also Table S1.†

SNAPol-1 entry into nuclei, possibly *via* the nuclear pore complex and also through detergent-induced membrane perturbations.[56]

Analysis of individual residues (Fig. 4A) confirmed the global increase in S/N, revealed the appearance of novel correlations for previously assigned residues (*e.g.*, T66 – Cγ), and increased the number of assigned residues to a total of 49 (Fig. 4B). It is evident from Fig. 4A that residues exhibited variations in Cα intensity (in cell *versus* in nuclei) and varying degrees of chemical shift (CS) perturbations (*e.g.*, E18) which suggested

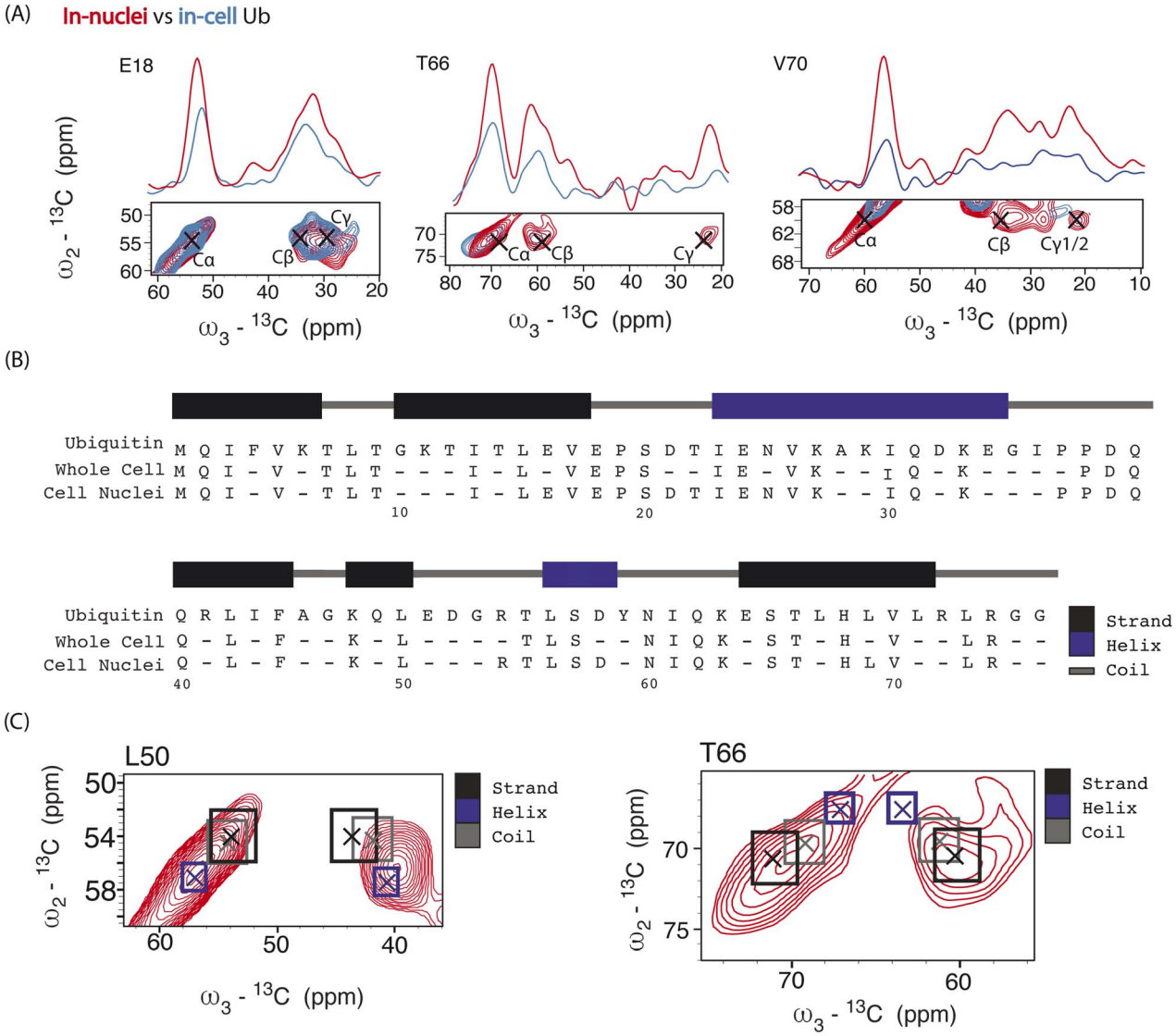

Fig. 4 Panel (A) overlay of aliphatic 2D projections and 1D slices extracted from ^{13}C–^{13}C–^{13}C DQSQSQ 3D experiment conducted at 800 MHz on 8 million HeLa cells (blue) electroporated with 1.2 mM [^{13}C,^{15}N]-Ub and on 1.6 × 10^7 isolated cell nuclei (red), both doped with 30 mM SNAPol-1. Black crosses denote literature assignments (BMRB ID: 15410 and 7111). Panel (B) sequence showing the assigned Ub residues at 800 MHz in isolated cell nuclei (49 residues) *versus* whole cells (41 resides). Panel (C) comparison of experimental 2D projections for L50 and T66 Cα/β overlayed with literature secondary chemical-shift values (with crosses denoting the average secondary structure chemical-shift) taken from ref. 57.

the presence of multiple Ub conformers. The observed variation in Ub's linewidth in cell *versus* microcrystals further substantiates this hypothesis. For example, while the (Cα,Cβ) cross peak correlation for L50 was dominated by α-helical conformations, we observed a broader distribution of (Cα, Cβ) correlations for T66 matching both β-sheet and random coil secondary structure values (Fig. 4C). The latter observation agrees with previous *in vitro* solution-state NMR studies suggesting that T66 adopts both β-sheet and random coil secondary structure.[48] Taken together these observations suggest that the increased spectral resolution and sensitivity seen in our 800 MHz DNP-ssNMR in cell and in nuclei data not only facilitate structural analysis, but also enable the study of conformational heterogeneity, that so far was mainly studied by *in vitro* solid-state NMR.[58,59]

Conclusion

Both sensitivity and resolution are critical for increasing the wide-spread use of in-cell DNP-ssNMR. Here we have shown that SNAPol-1 enables high field DNP-ssNMR for cellular applications not only with superior sensitivity but also leads to enhanced spectral resolution in a complex cellular setting and for a protein known to engage a multitude of intermolecular interactions.[60] A combination of microscopy and in-cell ssNMR data showed that SNAPol-1 readily enters and homogeneously distributes inside whole cells and isolated cell nuclei. By using HeLa cells containing near physiological concentrations of [^{13}C,^{15}N] Ub and doped with SNAPol-1, we observed significant improvements in resolution that approach data quality seen on

in vitro microcrystalline biological preparations. Further, we have expanded the scope of DNP-ssNMR to conduct experiments on intact nuclei. The physical removal of the cytoplasm facilitated improved SNAPol-1 entry and enabled data acquisition on the nuclear Ub pool with a 4-fold reduction in measurement time. A preliminary comparison of the resulting ssNMR correlations (Fig. 4) between in cell and in nuclei Ub spectra suggests that a multitude of Ub conformers can exist inside cells. Importantly, unlike in cell solution-state NMR which probes mostly monomeric conformers,[11,25,39] our presented approach probes all species,[41,61] regardless of molecular size, thus laying a foundation to comprehensively probe conformational protein states with sub-cellular selectivity.

Data availability

The data that support the findings of this study are available from the corresponding author upon reasonable request.

Author contributions

D. B., G. E. F., and M. B. designed experiments, analysed data, and wrote the manuscript. D. B. produced protein, samples, conducted confocal microscopy, and NMR experiments. M. K. assisted in confocal microscopy acquisition and analysis. A. G. maintained DNP instrumentation and A. S. assisted in Ub production. R. Y., X. C. and Y. L. produced synthetic SNAPol-1 and FITC-SNAPol-1. F. D., and M. P. C. M. produced TAMRA-Ub. All authors reviewed the manuscript and agreed to its publication.

Conflicts of interest

The authors have no conflicts to declare.

Acknowledgements

We thank Johan van der Zwan for technical support, Prof. Dr A. J. J. M. Bonvin for helpful discussions, and Dr Ilya Grigoriev of the Biology Imaging Center (BIC), Department of Biology, Utrecht University for confocal microscopy access and training. This work was supported by the Dutch Science Foundation NWO (grants 175.010.2009.002, 718.015.001 and 711.018.008 to M. B.) and by uNMR-NL-grid, a distributed state-of-the-art Magnetic Resonance Facility for the Netherlands (grant 184.035.002). In addition, our work was funded in part by iNEXT-Discovery (grant number 871037), a Horizon 2020 program of the European Commission, and the National Natural Science Foundation of China (No. 21871210, 22174099, and 21572161 to Y. P. L). F. D. acknowledges support from the European Union's Horizon 2020 research and innovation programme under the Marie Skłodowska-Curie grant agreement no. 813599. And M. P. C. M. acknowledges support from NWO (VIDI Grant VI. 213.110). The graphical abstract was prepared with Bio-render software.

Notes and references

1 P. G. Heytler and W. W. Prichard, *Biochem. Biophys. Res. Commun.*, 1962, **7**, 272–275.
2 J. Llopis, J. M. McCaffery, A. Miyawaki, M. G. Farquhar and R. Y. Tsien, *Proc. Natl. Acad. Sci. U. S. A.*, 1998, **95**, 6803–6808.
3 J. Davoust, J. Gruenberg and K. E. Howell, *EMBO J.*, 1987, **6**, 3601–3609.
4 N. H. Cho, K. C. Cheveralls, A.-D. Brunner, K. Kim, A. C. Michaelis, P. Raghavan, H. Kobayashi, L. Savy, J. Y. Li, H. Canaj, J. Y. S. Kim, E. M. Stewart, C. Gnann, F. McCarthy, J. P. Cabrera, R. M. Brunetti, B. B. Chhun, G. Dingle, M. Y. Hein, B. Huang, S. B. Mehta, J. S. Weissman, R. Gómez-Sjöberg, D. N. Itzhak, L. A. Royer, M. Mann and M. D. Leonetti, *Science*, 2022, **375**, eabi6983.
5 E. Lundberg and G. H. H. Borner, *Nat. Rev. Mol. Cell Biol.*, 2019, **20**, 285–302.
6 M. Mattiazzi Usaj, E. B. Styles, A. J. Verster, H. Friesen, C. Boone and B. J. Andrews, *Trends Cell Biol.*, 2016, **26**, 598–611.
7 F.-X. Theillet, A. Binolfi, B. Bekei, A. Martorana, H. M. Rose, M. Stuiver, S. Verzini, D. Lorenz, M. van Rossum, D. Goldfarb and P. Selenko, *Nature*, 2016, **530**, 45–50.
8 L. Barbieri, E. Luchinat and L. Banci, *Biochim. Biophys. Acta*, 2014, **1843**, 2492–2496.
9 R. Hänsel, L. M. Luh, I. Corbeski, L. Trantirek and V. Dötsch, *Angew Chem. Int. Ed. Engl.*, 2014, **53**, 10300–10314.
10 P. Broft, S. Dzatko, M. Krafcikova, A. Wacker, R. Hänsel-Hertsch, V. Dötsch, L. Trantirek and H. Schwalbe, *Angew. Chem., Int. Ed.*, 2021, **60**, 865–872.
11 K. Inomata, A. Ohno, H. Tochio, S. Isogai, T. Tenno, I. Nakase, T. Takeuchi, S. Futaki, Y. Ito, H. Hiroaki and M. Shirakawa, *Nature*, 2009, **458**, 106–109.
12 B. M. Burmann, J. A. Gerez, I. Matečko-Burmann, S. Campioni, P. Kumari, D. Ghosh, A. Mazur, E. E. Aspholm, D. Šulskis, M. Wawrzyniuk, A. Schmidt, S. G. D. Rüdiger, R. Riek and S. Hiller, *Nature*, 2020, **577**, 127–132.
13 S. Reckel, J. J. Lopez, F. Löhr, C. Glaubitz and V. Dötsch, *ChemBioChem*, 2012, **13**, 534–537.
14 L. A. Baker, T. Sinnige, P. Schellenberger, J. de Keyzer, C. A. Siebert, A. J. M. Driessen, M. Baldus and K. Grünewald, *Structure*, 2018, **26**, 161–170.
15 S. Chordia, S. Narasimhan, A. Lucini Paioni, M. Baldus and G. Roelfes, *Angew. Chem., Int. Ed.*, 2021, **60**, 5913–5920.
16 M. Kaplan, S. Narasimhan, C. de Heus, D. Mance, S. van Doorn, K. Houben, D. Popov-Čeleketić, R. Damman, E. A. Katrukha, P. Jain, W. J. C. Geerts, A. J. R. Heck, G. E. Folkers, L. C. Kapitein, S. Lemeer, P. M. P. van Bergen En Henegouwen and M. Baldus, *Cell*, 2016, **167**, 1241–1251.
17 Q. Z. Ni, E. Daviso, T. V. Can, E. Markhasin, S. K. Jawla, T. M. Swager, R. J. Temkin, J. Herzfeld and R. G. Griffin, *Acc. Chem. Res.*, 2013, **46**, 1933–1941.

18 M. Kaplan, A. Cukkemane, G. C. P. van Zundert, S. Narasimhan, M. Daniëls, D. Mance, G. Waksman, A. M. J. J. Bonvin, R. Fronzes, G. E. Folkers and M. Baldus, *Nat. Methods*, 2015, **12**, 649–652.
19 A. Jantschke, E. Koers, D. Mance, M. Weingarth, E. Brunner and M. Baldus, *Angew. Chem., Int. Ed.*, 2015, **54**, 15069–15073.
20 K. K. Frederick, V. K. Michaelis, B. Corzilius, T.-C. Ong, A. C. Jacavone, R. G. Griffin and S. Lindquist, *Cell*, 2015, **163**, 620–628.
21 T. Viennet, A. Viegas, A. Kuepper, S. Arens, V. Gelev, O. Petrov, T. N. Grossmann, H. Heise and M. Etzkorn, *Angew. Chem., Int. Ed.*, 2016, **55**, 10746–10750.
22 B. J. Albert, C. Gao, E. L. Sesti, E. P. Saliba, N. Alaniva, F. J. Scott, S. Th. Sigurdsson and A. B. Barnes, *Biochemistry*, 2018, **57**, 4741–4746.
23 R. Damman, A. Lucini Paioni, K. T. Xenaki, I. Beltrán Hernández, P. M. P. van Bergen En Henegouwen and M. Baldus, *J. Biomol. NMR*, 2020, **74**, 401–412.
24 R. Ghosh, Y. Xiao, J. Kragelj and K. K. Frederick, *J. Am. Chem. Soc.*, 2021, **143**, 18454–18466.
25 S. Narasimhan, S. Scherpe, A. Lucini Paioni, J. van der Zwan, G. E. Folkers, H. Ovaa and M. Baldus, *Angew. Chem., Int. Ed.*, 2019, **58**, 12969–12973.
26 E. J. Koers, E. A. W. van der Cruijsen, M. Rosay, M. Weingarth, A. Prokofyev, C. Sauvée, O. Ouari, J. van der Zwan, O. Pongs, P. Tordo, W. E. Maas and M. Baldus, *J. Biomol. NMR*, 2014, **60**, 157–168.
27 R. Gupta, H. Zhang, M. Lu, G. Hou, M. Caporini, M. Rosay, W. Maas, J. Struppe, J. Ahn, I.-J. L. Byeon, H. Oschkinat, K. Jaudzems, E. Barbet-Massin, L. Emsley, G. Pintacuda, A. Lesage, A. M. Gronenborn and T. Polenova, *J. Phys. Chem. B*, 2019, **123**, 5048–5058.
28 M. Lu, M. Wang, I. V. Sergeyev, C. M. Quinn, J. Struppe, M. Rosay, W. Maas, A. M. Gronenborn and T. Polenova, *J. Am. Chem. Soc.*, 2019, **141**, 5681–5691.
29 B. Uluca, T. Viennet, D. Petrović, H. Shaykhalishahi, F. Weirich, A. Gönülalan, B. Strodel, M. Etzkorn, W. Hoyer and H. Heise, *Biophys. J.*, 2018, **114**, 1614–1623.
30 I. V. Sergeyev, B. Itin, R. Rogawski, L. A. Day and A. E. McDermott, *Proc. Natl. Acad. Sci. U. S. A.*, 2017, **114**, 5171–5176.
31 P. Fricke, D. Mance, V. Chevelkov, K. Giller, S. Becker, M. Baldus and A. Lange, *J. Biomol. NMR*, 2016, **65**, 121–126.
32 W. Liu, Y. Wang, L. H. M. Bozi, P. Fischer, M. P. Jedrychowski, H. Xiao, T. Wu, N. Darabedian, X. He, E. L. Mills, N. Burger, S. Shin, A. Reddy, H.-G. Sprenger, N. Tran, S. Winther, S. M. Hinshaw, J. Shen, H.-S. Seo, K. Song, A. Z. Xu, L. Sebastian, J. Zhao, S. Dhe-Paganon, J. Che, S. P. Gygi, H. Arthanari and E. T. Chouchani, *Nature*, 2023, 1–3.
33 J. Han and K. Burgess, *Chem. Rev.*, 2010, **110**, 2709–2728.
34 X. Cai, A. Lucini Paioni, A. Adler, R. Yao, W. Zhang, D. Beriashvili, A. Safeer, A. Gurinov, A. Rockenbauer, Y. Song, M. Baldus and Y. Liu, *Chem.–Eur. J.*, 2021, **27**, 12758–12762.
35 R. Yao, D. Beriashvili, W. Zhang, S. Li, A. Safeer, A. Gurinov, A. Rockenbauer, Y. Yang, Y. Song, M. Baldus and Y. Liu, *Chem. Sci.*, 2022, **13**, 14157–14164.
36 J. Liwocha, D. T. Krist, G. J. van der Heden van Noort, F. M. Hansen, V. H. Truong, O. Karayel, N. Purser, D. Houston, N. Burton, M. J. Bostock, M. Sattler, M. Mann, J. S. Harrison, G. Kleiger, H. Ovaa and B. A. Schulman, *Nat. Chem. Biol.*, 2021, **17**, 272–279.
37 P. C. A. van der Wel, K.-N. Hu, J. Lewandowski and R. G. Griffin, *J. Am. Chem. Soc.*, 2006, **128**, 10840–10846.
38 A. M. Vian and A. Z. Higgins, *Cryobiology*, 2014, **68**, 35–42.
39 W. Zhu, A. J. Guseman, F. Bhinderwala, M. Lu, X.-C. Su and A. M. Gronenborn, *Angew. Chem., Int. Ed.*, 2022, **61**, e202201097.
40 H. Kadavath, N. C. Prymaczok, C. Eichmann, R. Riek and J. A. Gerez, *Angew. Chem., Int. Ed.*, 2023, **62**, e202213976.
41 S. E. Kaiser, B. E. Riley, T. A. Shaler, R. S. Trevino, C. H. Becker, H. Schulman and R. R. Kopito, *Nat. Methods*, 2011, **8**, 691–696.
42 H. Heise, K. Seidel, M. Etzkorn, S. Becker and M. Baldus, *J. Magn. Reson.*, 2005, **173**, 64–74.
43 A. B. Barnes, B. Corzilius, M. L. Mak-Jurkauskas, L. B. Andreas, V. S. Bajaj, Y. Matsuki, M. L. Belenky, J. Lugtenburg, J. R. Sirigiri, R. J. Temkin, J. Herzfeld and R. G. Griffin, *Phys. Chem. Chem. Phys.*, 2010, **12**, 5861–5867.
44 B. Corzilius, L. B. Andreas, A. A. Smith, Q. Z. Ni and R. G. Griffin, *J. Magn. Reson.*, 2014, **240**, 113–123.
45 A. H. Linden, W. T. Franks, Ü. Akbey, S. Lange, B.-J. van Rossum and H. Oschkinat, *J. Biomol. NMR*, 2011, **51**, 283.
46 C. A. Castañeda, E. K. Dixon, O. Walker, A. Chaturvedi, M. A. Nakasone, J. E. Curtis, M. R. Reed, S. Krueger, T. A. Cropp and D. Fushman, *Structure*, 2016, **24**, 423–436.
47 M. K. Hospenthal, S. M. V. Freund and D. Komander, *Nat. Struct. Mol. Biol.*, 2013, **20**, 555–565.
48 C. Gladkova, A. F. Schubert, J. L. Wagstaff, J. N. Pruneda, S. M. Freund and D. Komander, *EMBO J.*, 2017, **36**, 3555–3572.
49 O. F. Lange, N.-A. Lakomek, C. Farès, G. F. Schröder, K. F. A. Walter, S. Becker, J. Meiler, H. Grubmüller, C. Griesinger and B. L. de Groot, *Science*, 2008, **320**, 1471–1475.
50 L. Sardo, A. Lin, S. Khakhina, L. Beckman, L. Ricon, W. Elbezanti, T. Jaison, H. Vishwasrao, H. Shroff, C. Janetopoulos and Z. A. Klase, *J. Cell Sci.*, 2017, **130**, 2926–2940.
51 B. A. Maxwell, Y. Gwon, A. Mishra, J. Peng, H. Nakamura, K. Zhang, H. J. Kim and J. P. Taylor, *Science*, 2021, **372**, eabc3593.
52 K. Juenemann, A. H. P. Jansen, L. van Riel, R. Merkx, M. P. C. Mulder, H. An, A. Statsyuk, J. Kirstein, H. Ovaa and E. A. Reits, *Sci. Rep.*, 2018, **8**, 1405.
53 N. P. Dantuma, T. A. M. Groothuis, F. A. Salomons and J. Neefjes, *J. Cell Biol.*, 2006, **173**, 19–26.
54 E. Wist and H. Krokan, *Exp. Cell Res.*, 1978, **116**, 313–316.
55 R. S. D. Read and C. M. Mauritzen, *Can. J. Biochem.*, 1970, **48**, 559–565.

56 K. E. Knockenhauer and T. U. Schwartz, *Cell*, 2016, **164**, 1162–1171.
57 Y. Wang and O. Jardetzky, *Protein Sci.*, 2002, **11**, 852–861.
58 H. Heise, S. Luca, B. L. de Groot, H. Grubmüller and M. Baldus, *Biophys. J.*, 2005, **89**, 2113–2120.
59 R. H. Havlin and R. Tycko, *Proc. Natl. Acad. Sci. U. S. A.*, 2005, **102**, 3284–3289.
60 I. Dikic and B. A. Schulman, *Nat. Rev. Mol. Cell Biol.*, 2022, 1–15.
61 K. N. Swatek, J. L. Usher, A. F. Kueck, C. Gladkova, T. E. T. Mevissen, J. N. Pruneda, T. Skern and D. Komander, *Nature*, 2019, **572**, 533–537.